IEEE Access
Multidisciplinary | Rapid Review | Open Access Journal

Received October 22, 2017, accepted November 16, 2017, date of publication December 6, 2017,
date of current version February 14, 2018.

Digital Object Identifier 10.1109/ACCESS.2017.2779107

Feature Enhancement in Visually Impaired Images

MADHURI SUTHAR[1], (Student Member, IEEE), HOSSEIN ASGHARI[2], AND BAHRAM JALALI[3,4,5,6], (Fellow, IEEE)

[1]Department of Electrical and Computer Engineering, University of California at Los Angeles, Los Angeles, CA 90095, USA
[2]Department of Electrical Engineering and Computer Science, Loyola Marymount University, Los Angeles, CA 90045, USA
[3]Department of Electrical and Computer Engineering David Geffen School of Medicine, University of California at Los Angeles, Los Angeles, CA 90095, USA
[4]Department of Bioengineering, David Geffen School of Medicine, University of California at Los Angeles, Los Angeles, CA 90095, USA
[5]Department of Surgery, David Geffen School of Medicine, University of California at Los Angeles, Los Angeles, CA 90095, USA
[6]California NanoSystems Institute, Los Angeles, CA 90095, USA

Corresponding author: Madhuri Suthar (madhurisuthar@ucla.edu)

This work was supported in part by the National Institutes of Health under Grant 5R21 GM107924-03 and in part by the Office of Naval Research Multidisciplinary University Research Initiatives program on Optical Computing under Award N00014-14-1-0505.

ABSTRACT One of the major open problems in computer vision is feature detection in visually impaired images. In this paper, we describe a potential solution using phase stretch transform, a new computational approach for image analysis, edge detection and resolution enhancement that is inspired by the physics of the photonic time stretch technique. We mathematically derive the intrinsic nonlinear transfer function and demonstrate how it leads to: 1) superior performance at low contrast levels and 2) a reconfigurable operator for hyper-dimensional classification. We prove that the phase stretch transform equalizes the input image brightness across a range of intensities resulting in high dynamic range in visually impaired images. We also show further improvement in the dynamic range by combining our method with the conventional techniques. Finally, our results propose a new paradigm for the computation of mathematical derivatives via group delay dispersion operations.

INDEX TERMS Phase stretch transform, image edge detection, dynamic range, feature enhancement, image analytics, feature detection, feature extraction, image processing, computer vision.

I. INTRODUCTION

Feature detection in images plays a critical role in the field of computer vision for solving problems associated with object recognition, image registration, content-based image retrieval and deep learning [1]–[3]. Prior works for improving feature detection in images have focused on the use of grey level statistics of the image [1] and on application of edge detection methods [4]. Color distinctiveness and color models [5], [6] and scale selections [7] in images have also been exploited for enhancing the feature detection. The main goal of feature detection is to classify objects more accurately and at the same time be robust to varying viewing conditions that include changes in illumination, environmental conditions, object orientation, and the zoom factor of the camera. Environmental conditions can severely impair detection and localization of objects in images. For instance, under foggy conditions, acquired images suffer from visual impairments such as reduced contrast, blur and noise which leads to lower resolution [8], [9]. This constitutes a major bottleneck for many computer vision applications including autonomous vehicles. The emerging imaging technologies such as High Dynamic Range (HDR) hold promise to solve feature detection problems but their slow frame rate pose a challenge in real-time applications such as self-driven cars and autonomous robotics.

The Phase Stretch Transform (PST) was recently introduced as a computational approach for signal and image processing [10], [11]. PST is a physics-based algorithm that has its roots in photonic time stretch technique [12]–[16], a method for real-time measurements of ultra-fast events and one that has enabled the discovery of optical rogue waves [17], observation of relativistic electron structure [18], label-free cancer cell detection with record accuracy [19], [20] and optical data compression [21]. The algorithm mimics the propagation of electromagnetic waves through a diffractive medium with engineered 3D dispersive property (refractive index) [10], [11]. As introduced in [22], this optics-inspired algorithm has superior properties that can be exploited to develop advanced algorithms for feature extraction from digital images. Here, we discuss in detail the nonlinear behavior of PST and demonstrate how this behavior can be used to solve problems related to feature detection for

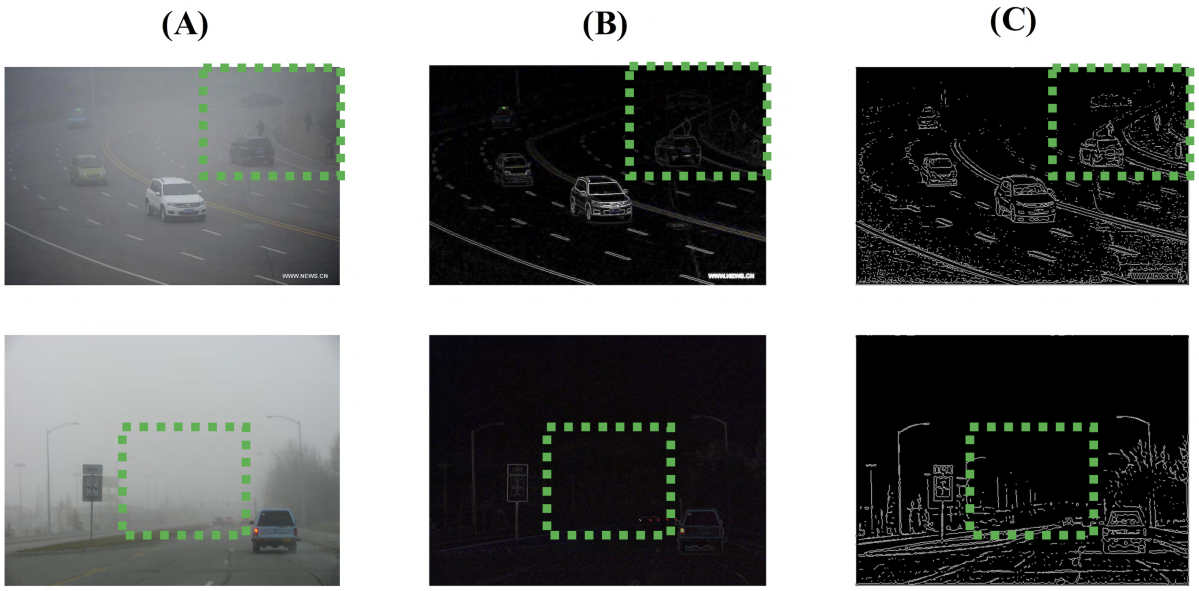

FIGURE 1. Comparison of feature detection using the conventional derivative operator and feature detection using PST in case of visually impaired images. The original images were taken under foggy conditions, shown in (A). Results of feature detection using the conventional derivative operator and the PST operator are shown in (B) and (C), respectively. Note that the conventional derivative operator fails to efficiently visualize the low contrast features in the visually impaired regions of the images (shown in green dashed boxes). However, PST captures these low contrast features in the low resolution regions of the image (shown in green dashed boxes) due to its reconfigurable mechanism that enables feature detection over a wide dynamic range.

computer vision applications. PST can be applied to both digital images as well as time series data [23] and has been used for edge detection in biomedical images [11], [24] and Synthetic Aperture Radar (SAR) images [25]. PST has also been applied for resolution enhancement in super-resolution localization microscopy for imaging of a single molecule [26]. The algorithm has been open sourced on GitHub and Matlab Central File Exchange [27].

We first show that PST has an inherent equalization ability that gives a response ideal for feature detection in low contrast regimes of visually impaired images. To do this, we apply our edge detection algorithm on two road traffic images taken under foggy conditions, as shown in Fig. 1. The figure depicts how our edge detection algorithm could significantly improve the feature detection in case of visually impaired images by outperforming the conventional edge detection methods based on derivative of the image. The conventional derivative based method is unable to capture details with small contrast in the brighter low resolution areas of the image whereas our technique successfully detects features in these low contrast visually impaired regions. The warp and strength parameters of the PST kernel as described in [10] and [11] for feature detection in these images are 22 and 500, respectively. As we will show in our mathematical formulations, this property emerges because PST's transfer function is a reconfigurable operator. Finally, we demonstrate the superior performance of PST at low light levels and its application to HDR images.

II. MATHEMATICAL FOUNDATIONS OF PHASE STRETCH TRANSFORM

We prove the superior performance of Phase Stretch Transform in the low contrast regime by deriving closed-form analytical expressions for its transfer function. Mathematical results reveal that the transform has an intrinsic intensity equalization property that leads to high dynamic range performance. Analytical results are supported by numerical simulations confirming the dynamic range enhancement. We define the stretch operator $\mathbb{S}\{\}$ as follows:

$$\begin{aligned} E_o[x,y] &= \mathbb{S}\{E_i[x,y]\} \\ &\triangleq IFFT2\left\{\widetilde{K}[u,v]\cdot\widetilde{L}[u,v]\cdot FFT2\{E_i[x,y]\}\right\} \end{aligned} \quad (1)$$

where $E_o[x,y]$ is a complex quantity defined as,

$$E_o[x,y] = |E_o[x,y]|\ e^{j\theta[x,y]} \quad (2)$$

In the above equations, $E_i[x,y]$ is the input image, x and y are the spatial variables, FFT2 is the two-dimensional Fast Fourier Transform, IFFT2 is the two-dimensional Inverse Fast Fourier Transform, and u and v are frequency variables. The function $\widetilde{K}[u,v]$ is called the warped phase kernel and the function $\widetilde{L}[u,v]$ is a localization kernel implemented in frequency domain. Here, for simplicity we assume $\widetilde{L}[u,v]=1$.

The PST operator is defined as the phase of the Warped Stretch Transform output as follows,

$$PST\left\{E_i[x,y]\right\} \triangleq \measuredangle\left\{S\{E_i[x,y]\}\right\} \quad (3)$$

where $\measuredangle\langle\cdot\rangle$ is the angle operator.

Without loss of generality and in order to keep the notations manageable in what follows, we consider the operation of PST on 1D data, i.e.,

$$\begin{aligned} PST\left\{E_i[x]\right\} &= \measuredangle\left\{E_o[x]\right\} \\ &= \measuredangle\left\langle IFFT\left\{\widetilde{K}[u]\cdot FFT\{E_i[x]\}\right\}\right\rangle \end{aligned} \quad (4)$$

The warped phase kernel $\widetilde{K}[u]$ is described by a phase function with a nonlinear dependence on the frequency variable, u,

$$\widetilde{K}[u] = e^{j\cdot\phi[u]} \tag{5}$$

By using the Taylor expansion for the phase term in the warped phase kernel $\widetilde{K}[u]$, we have:

$$\widetilde{K}[u] = e^{\left(j\sum_{m=2}^{M}\frac{\phi^{(m)}}{m!}u^m\right)} \tag{6}$$

where $\phi^{(m)}$ is the mth- order discrete derivative of the phase $\phi[u]$ evaluated for $u = 0$ and values of m are even numbers. PST phase term $\phi[u]$ only contains even-order terms in its Taylor expansion due to even symmetry of the phase term $\phi[u]$ considered in [10] and [11]. Using the warped phase kernel described in equation (6), output complex-field, $E_o[x]$, can be calculated as follows,

$$\begin{aligned} E_o[x] &= IFFT\left\{\widetilde{E}_i[u] \times \widetilde{K}[u]\right\} \\ &= IFFT\left\{\widetilde{E}_i[u] \times e^{\left(j\sum_{m=2}^{M}\frac{\phi^{(m)}}{m!}u^m\right)}\right\} \end{aligned} \tag{7}$$

where $\widetilde{E}_i[u]$ is the discrete Fourier transform of the input. Simulations show that PST works best when the applied phase is small. Under these conditions, using small value approximation for the applied phase kernel, the exponential term in (7) can be simplified to,

$$E_o[x] = IFFT\left\{\widetilde{E}_i[u] \times \left[1 + j\left(\sum_{m=2}^{M}\frac{\phi^{(m)}}{m!}u^m\right)\right]\right\} \tag{8}$$

$$\rightarrow E_o[x] \approx \left[1 \times E_i[x] + j\sum_{m=2}^{M}\frac{(-1)^{m/2}\,\phi^{(m)}}{m!\;(2\pi)^m}E_i[x]^{(m)}\right] \tag{9}$$

where $E_i[x]^{(m)}$ is the mth-order discrete derivative of the input $E_i[x]$. Since the input is a real quantity, the output phase can be calculated as,

$$\begin{aligned} PST\{E_i[x]\} &= \measuredangle\{E_o[x]\} \\ &\approx \tan^{-1}\left\{\frac{\sum_{m=2}^{M}\frac{(-1)^{m/2}\,\phi^{(m)}}{m!\;(2\pi)^m}E_i[x]^{(m)}}{E_i[x]}\right\} \end{aligned} \tag{10}$$

Finally, since the phase is restricted to small values, (10) can be simplified to,

$$PST\{E_i[x]\} \approx \left\{\frac{\sum_{m=2}^{M}\frac{(-1)^{m/2}\,\phi^{(m)}}{m!\;(2\pi)^m}E_i[x]^{(m)}}{E_i[x]}\right\} \tag{11}$$

We see that the transfer function consists of a summation of even-order derivatives in the numerator divided by the amplitude (brightness) in the denominator. The numerator extracts a hyper-dimensional set of features that corresponds to different measures of the curvature of the edge. The denominator renders the response nonlinear in such a way that low light levels are enhanced. These results were obtained for a general phase kernel and for small values of phase in the PST kernel. We now consider two additional scenarios that reveal further insight into the unique properties of our transform.

Case 1: We consider the Phase Kernel $\widetilde{K}[u] = u^2$ as a quadratic function of frequency variable u. Under this condition, using small phase approximation as used before, the exponential term in (8) can be simplified to,

$$E_o[x] = IFFT\left\{\widetilde{E}_i[u] \times \left[1 + j\left(u^2\right)\right]\right\} \tag{12}$$

$$\rightarrow E_o[x] \approx \left[1 \times E_i[x] - j\frac{1}{(2\pi)^2} * \frac{d^2E_i[x]}{dx^2}\right] \tag{13}$$

Finally, for calculating the phase of the complex output we assume it to be restricted to small values. Therefore, the phase of the output in equation (13) can be simplified to,

$$PST\{E_i[x]\} = \measuredangle E_o[x] \approx \frac{\frac{-1}{(2\pi)^2} * \frac{d^2E_i[x]}{dx^2}}{E_i[x]} \tag{14}$$

Case 2: Here we consider, the same Phase Kernel $\widetilde{K}[u] = u^2$ as a quadratic function of frequency variable u as discussed in Case 1. However, we remove the use of small phase approximation. The exponential term in (8) now leads to,

$$E_o[x] = IFFT\left\{\widetilde{E}_i[u] \times \left[\cos\left(u^2\right) + j\,sin\left(u^2\right)\right]\right\} \tag{15}$$

Expanding the sine and cosine terms using Euler expansion up to third order and then applying small value approximation to the complex output of (12) will result in the PST output as shown below

$$\begin{aligned} &PST\{E_i[x]\} \\ &= \measuredangle E_o[x] \\ &\approx \frac{\frac{-1}{(2\pi)^2} * \frac{d^2E_i[x]}{dx^2} + \frac{1}{3!(2\pi)^6} * \frac{d^6E_i[x]}{dx^6} - \frac{1}{5!(2\pi)^{10}} * \frac{d^{10}E_i[x]}{dx^{10}}}{E_i[x] - \frac{1}{2!(2\pi)^4} * \frac{d^4E_i[x]}{dx^4} + \frac{1}{4!(2\pi)^8} * \frac{d^8E_i[x]}{dx^8}} \end{aligned} \tag{16}$$

The closed-form expression presented in the equation (11) relates the output to the input in the case of a arbitrary phase kernel with small phase approximation. The core functionality of the PST as a feature detector can be understood by closed-form expression shown in (11). The output of the PST operator is related directly to the even-order derivatives of the input with weighing factors of $\frac{(-1)^{m/2}\,\phi^{(m)}}{m!\;(2\pi)^m}$. Each derivatives detects a different feature in the input. Thus, the weighing factors can be designed to select features of interest. In other words, our transform is a reconfigurable operator that can be tuned to emphasize different features in an input image.

The important observation from (11) is that, the output is inversely related to the input brightness level, and this is valid for small phase approximation. Therefore, for the same contrast level, the output is larger in low light level

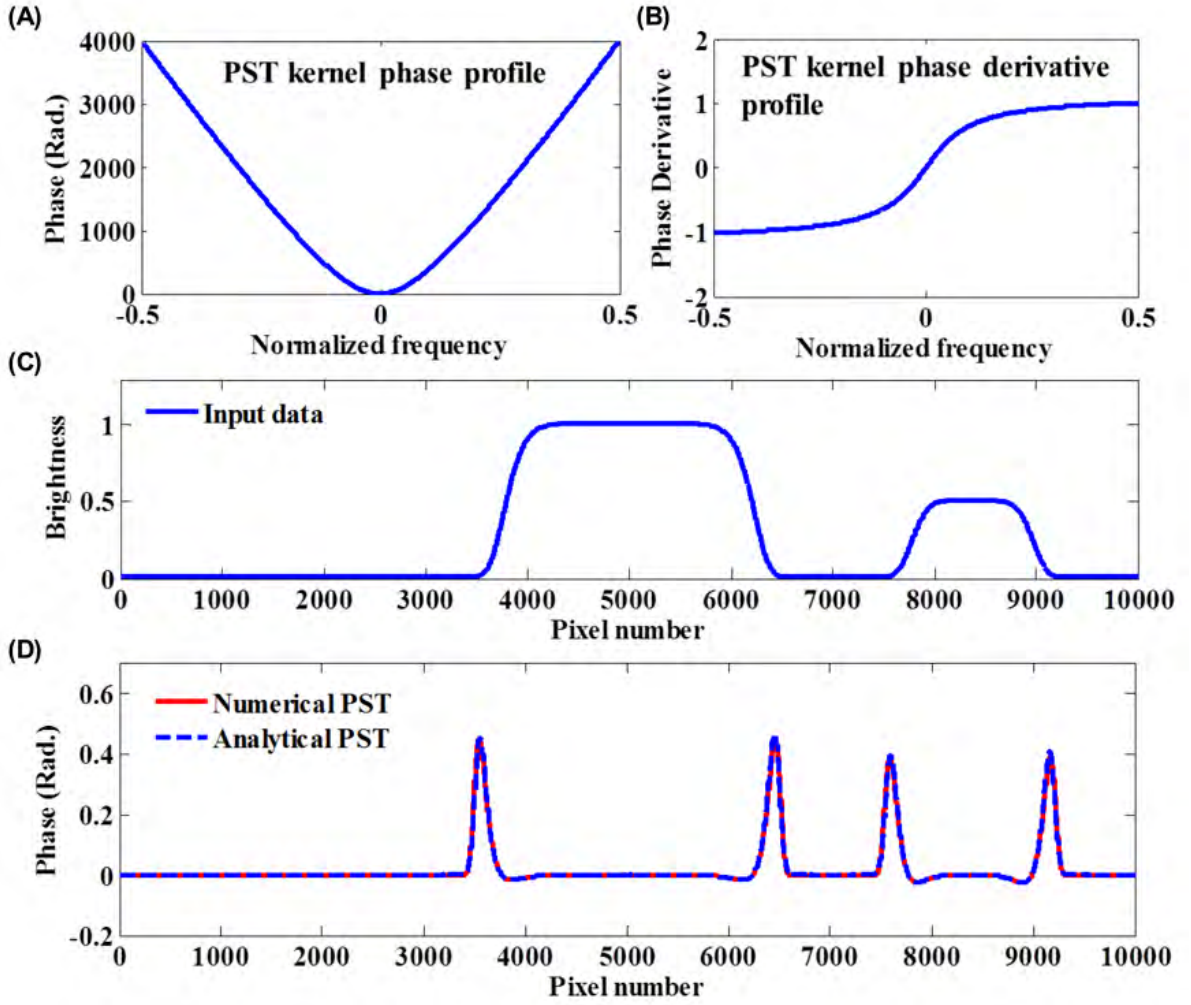

FIGURE 2. Comparison of the numerically simulated output of the PST algorithm with the output given by the closed-form analytical expression derived in Equation (11). The phase kernel and the corresponding phase derivative profile are shown in (A) and (B), respectively. The input 1D brightness data simulated for the comparison is shown in (C). Numerically calculated output data is compared to the analytical output data estimated by (11) in (D) using red-solid and blue-dotted lines, respectively. Simulation results validate the accuracy of the closed-form analytical model given by Equation (11).

regions of the image. This crucial property, inherent to PST, equalizes the input brightness and allows for more sensitive feature detection and enhancement. Brightness level equalization is a well-studied method to improve feature detection algorithms in High Dynamic Range (HDR) images (see [28] for an example). One technique for brightness level equalization in images is a log function applied to the input before feature detection. The log function has a higher gain for lower brightness input which equalizes the brightness and results in more efficient feature detection. Fortunately, the PST operator has a built-in logarithmic behavior which gives it excellent dynamic range. However, this does not completely describe the transform. As observed in Equation (16), our transform outputs a hyper-dimensional feature set for classification. These results also show a method for the computation of mathematical derivatives via group delay dispersion operations.

III. SIMULATION RESULTS

In this section, we present some simulation results that validate the closed-form expression derived in the previous section. We also show examples of the operation of PST on HDR images, supporting the new theory developed above. In the first example, we simulate the output for a given 1D data and compare it to the output estimated by the mathematical expression derived in Equation (11). The phase kernel $\phi[u]$ constructed for the PST operator is shown in Fig. 2(A). The warp and strength parameters of the kernel as described in [10] and [11] are 12.5 and 4000, respectively. The phase and its derivative are shown in Fig. 2(A) and Fig. 2(B) respectively. The input is shown in Fig. 2(C). Numerically simulated output is compared to the output estimated by (11) in Fig. 2(D) using red-solid and blue-dotted lines, respectively. It is evident that the simulations match analytically derived results

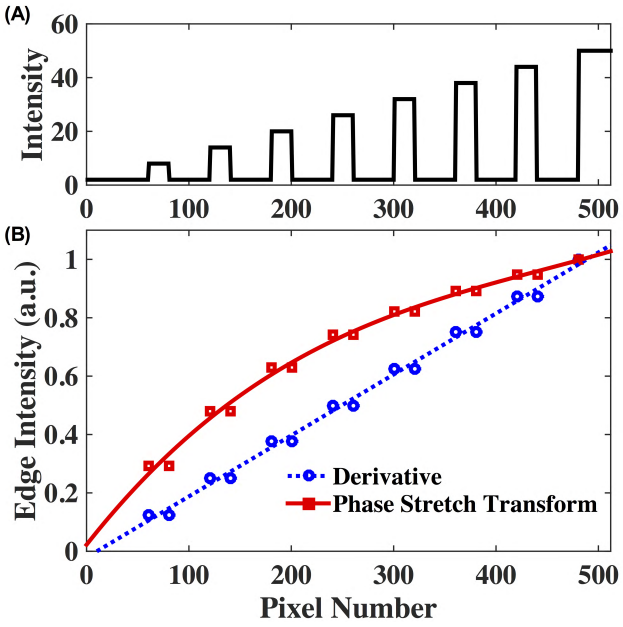

FIGURE 3. Effect of PST on features with varying contrast levels at a fixed brightness level compared to the output by differentiation. The input is shown in (A). The output of the differentiator (shown in blue-dotted lines) is linearly related to the contrast level and is insensitive to the brightness level. However, the dependence of the PST output (shown in red-dotted lines) to the contrast level at a fixed brightness level is nonlinear.

validating the accuracy of the closed-form analytical model of our algorithm.

In the next example, we evaluate the effect of PST on features with different contrast levels at a fixed brightness level and compare it to the case of using the conventional derivative technique to detect features in the same input. The warp and strength parameters used for the PST operator are 12.15 and 0.48, respectively. The input was designed to have different contrast levels at a fixed brightness level (see Fig. 3(A)). Numerically simulated output using PST is compared to the output using differentiation in Fig. 3(B). As expected, the output of the differentiator is linearly related to the contrast level and is insensitive to the brightness level. However, the relation of the PST output to the contrast level at a fixed brightness level is nonlinear. This effect is due to the brightness level equalization feature of PST described in equation (11).

Fig. 4 shows an example of using PST for feature enhancement in a 14-bit HDR image. The image has sharp features in the low contrast regions, as shown in the red boxes. Here we compare the feature detection using the derivative operator with that using PST. The derivative operator was implemented from native smooth derivative function. For fair comparison, both methods use the same localization kernel with sigma factor of 2 in all the experiment results shown here. The warp and strength parameters used for the PST operator are 12.15 and 0.48, respectively. Results of feature detection using the smooth derivative operator and the PST operator are shown in Fig. 4(B) and Fig. 4(C), respectively. The derivative operator is unable to unveil the low contrast features in the dark areas of the image, see dashed box in Fig. 4(B). However, PST extracts these low contrast features in the dark areas due to its natural equalization mechanism, see red boxes in Fig. 4(C). Also, it can

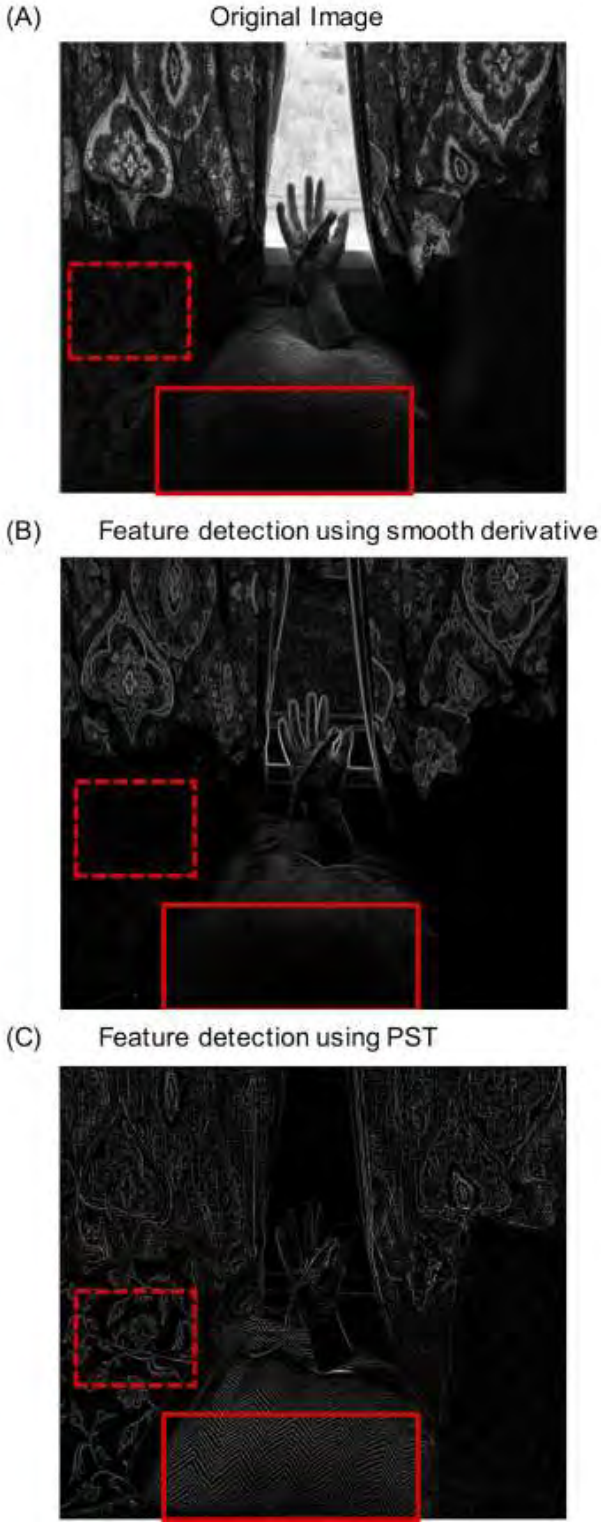

FIGURE 4. Comparison of feature detection using the smooth derivative operator to the case of feature detection using the PST. The original image is shown in (A). The smooth derivative operator is unable to efficiently visualize low contrast features in the dark areas of the image which are successfully captured by the PST operator.

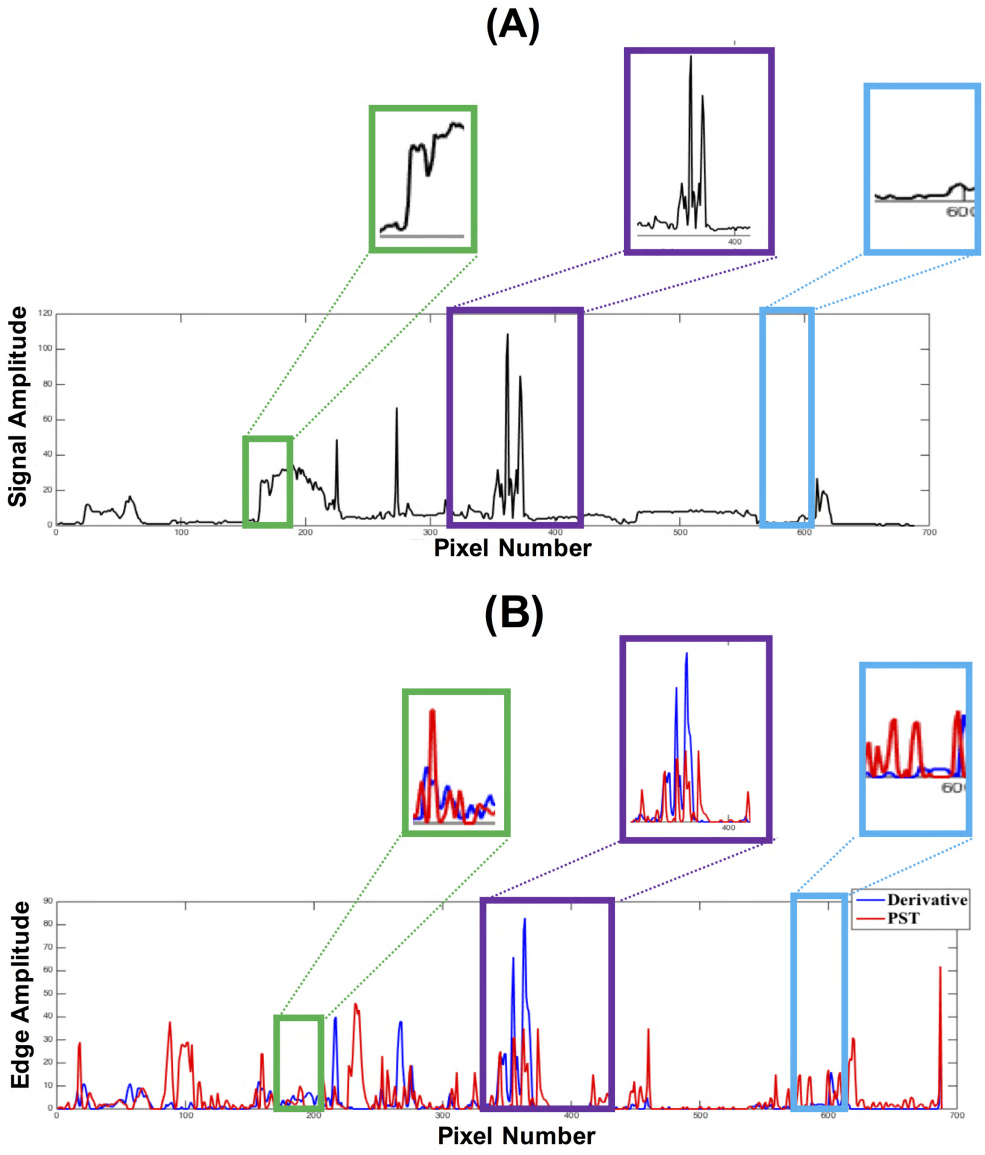

FIGURE 5. A line scan corresponding to row number 524 of the image previously shown in Fig. 4 that compares the feature detection output of the conventional derivative operator to that of the PST operator under low light level and high light level conditions. The original input line scan is shown in (A). Feature detection of this line scan using the derivative operator and the PST are shown in (B). PST operator is more sensitive than the derivative operator under low contrast conditions in both the low light level and high light level conditions (see purple and green box).

be observed that the intensity of detected edges in the case of smooth derivative is related linearly to the brightness level of the original image, compare solid box areas in Fig. 4(A) and Fig. 4(B). On the contrary, PST has automatically equalized the brightness level in the solid box region in the image and outputs relatively fixed features intensity for that region, see solid box in Fig. 4(C). It can be seen that PST has failed to visualize features in very bright areas of the image such as the edges of the hand. This is because of the inverse dependence on brightness as shown in (11). This problem can be solved by setting a maximum threshold for detected features or by equalizing the image brightness before applying the PST operator.

To better understand the role of PST for feature detection in low light level and high light level regions, we use a single line scan of the HDR image shown previously in Fig. 4. The blue box in the Fig. 5 demonstrates the response of PST to low light level regions where it outperforms conventional derivative operator. Similarly, for high light level regions of the image (shown in green and purple box in the Fig. 5), PST outperforms when the contrast is low (shown in green box in the Fig. 5). On the contrary, the conventional derivative operator response dominates only in high contrast regions (shown in purple box in the Fig. 5).

We consider another 14-bit HDR image to show feature enhancement in low light level regions using PST.

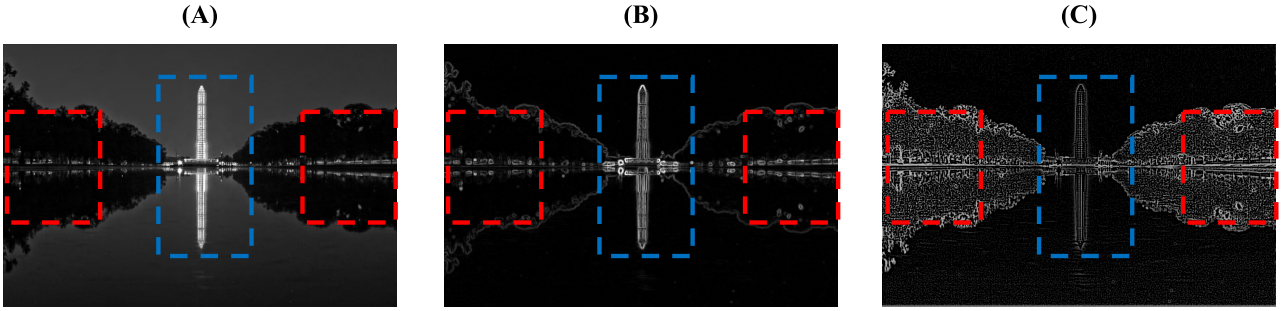

FIGURE 6. Comparison of feature detection using the smooth derivative operator to the case of feature detection using the PST. The original image is shown in (A). The smooth derivative operator is unable to efficiently visualize the features in the low contrast areas of the image (see red boxes in (B)) whereas PST detects these low contrast features (see red boxes in (C)).

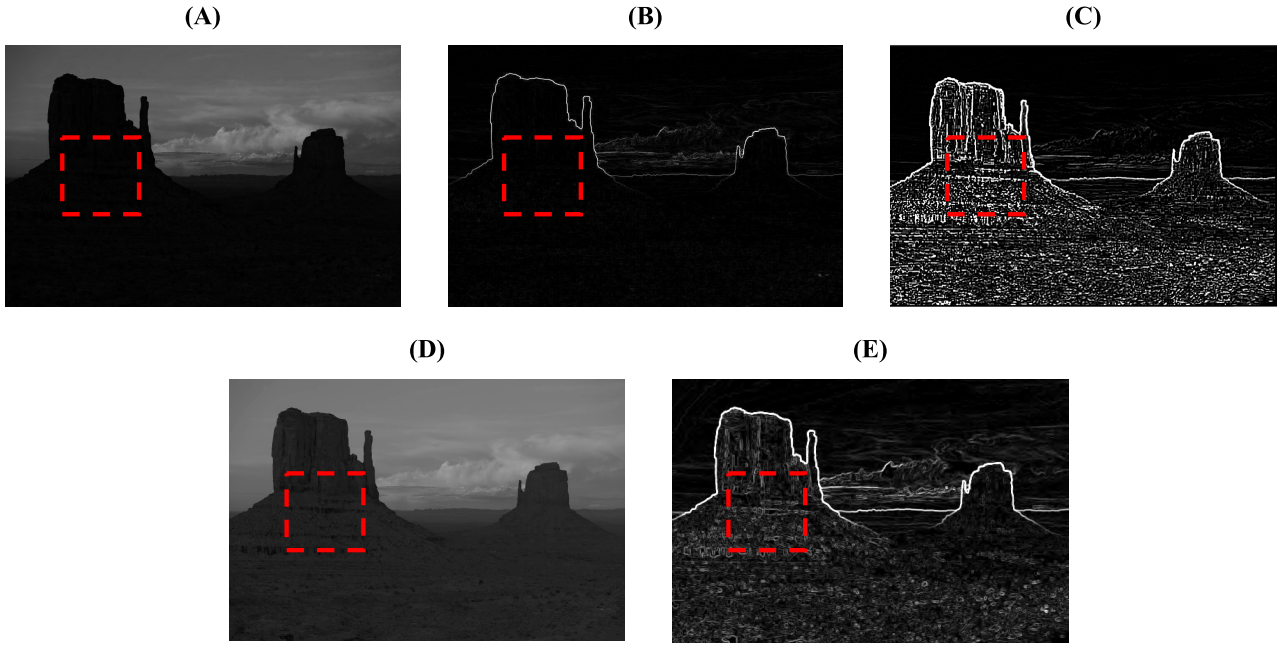

FIGURE 7. Comparison of feature detection using the smooth derivative operator on a contrast enhanced image to the case of feature detection using the PST. The original image is shown in (A). The smooth derivative operator detects features in the under-exposed regions of the image only after enhancing the contrast of the image. The edges detected by the conventional derivative operator in the under-exposed regions of the contrast enhanced image are consistent with the ones detected by the PST (see red boxes in (C) and (E)). (A) Original image (C) Feature detection using PST (D) Contrast Enhanced Image (E) Feature detection using conventional edge detectors on contrast enhanced image

The image has sharp features in the form of edges of leaves and branches of trees in the low light level regions, see red dashed box in Fig. 6(A). Results of feature detection using the smooth derivative operator and the PST operator are shown in Fig. 6(B) and Fig. 6(C), respectively. The warp and strength parameters used for the PST operator are 22.4 and 10.5, respectively. The conventional smooth derivative operator detects features only in high contrast regions, as shown in blue dashed box. The derivative operator fails to identify edges corresponding to low contrast areas of the image, see red dashed box in Fig. 6(B). PST due to its inherent equalization mechanism detects these features as shown in red dashed box in Fig. 6(C). It can be observed that PST does not have a strong edge response corresponding to high contrast regimes such as the edges of Washington Monument in the image. We will show later that this issue can be resolved by combining the edges from both the methods.

In order to evaluate the performance of PST compared to the previous methods, we show an example of using PST for feature enhancement in a 14-bit HDR image and then compare the output with the conventional techniques for feature enhancement in low contrast regions. The image of the rock has sharp surface variations in the low light level regions, as shown in the red dashed box. The smooth derivative operator fails to detect these surface features in low contrast regions, see Fig. 7(B). We apply the standard intensity histogram equalization technique [28] to enhance the contrast of the under-exposed regions of this HDR image, shown in Fig. 7(D). The derivative operator now detects features in these low contrast regions, see Fig. 7(E) which are visually consistent with the features detected by PST, see Fig. 7(C). The warp and strength parameters used for the PST operator are 12.4 and 0.48, respectively.

We consider another example of a defocused image, shown in Fig. 8(A), to show that PST outperforms conventional

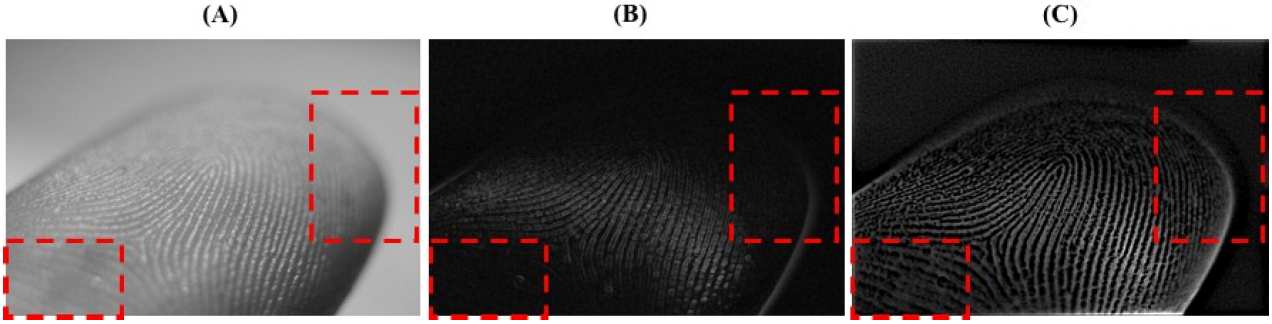

FIGURE 8. Comparison of feature detection using the smooth derivative operator to the case of feature detection using the PST operator. The original image is shown in (A). The smooth derivative operator is unable to detect features in the defocused areas of the image (as shown in red boxes in (B)). However, PST captures the fingerprint details in these blurred areas due to its unique reconfigurable property (see (C)).

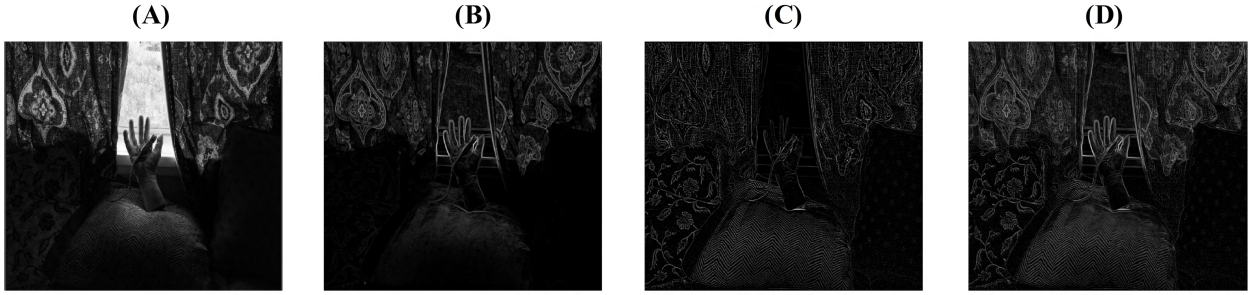

FIGURE 9. Hybrid system that combines the edge maps from the smooth derivative operator and the PST. The original image is shown in (A). Results of feature detection using the smooth derivative operator and the PST are shown in (B) and (C), respectively. The output of the hybrid system is shown in (D). Note that in (D), the strength of the detected features in both the high light level and low light level regions is same. The hybrid system selects the detected features in the darker regions using the PST and in the brighter regions using the smooth derivative operator and thereby, provides a wide dynamic range of operation.

edge detectors for feature enhancement in visually impaired images. By comparing the edge map from smooth derivative function to that from the PST operator, shown in Fig. 8(B) and Fig. 8(C), respectively, it is evident that the PST operator detects edges of finger prints in the blurred (low contrast) regions marked by red boxes. This opens up the possibility of using PST for fingerprint analysis in forensic science. The warp and strength parameters used here for the PST operator are 1000.2 and 50.4, respectively.

To further enhance the dynamic range of operation for feature detection, we introduce a hybrid system that combines the edge responses from the PST and the conventional derivative operator, enabling feature detection in low as well as high contrast regions. As shown in Fig. 9, the edge map of the hybrid system has edges in the high contrast regions such as the hand in the image and also in the low contrast regions such as the pattern on the curtain. It can be clearly seen that the feature detection of the hybrid system surpasses the capabilities of feature detection from the derivative and the PST operator.

IV. CONCLUSIONS

In this paper, we presented a new method for edge detection in visually impaired images using a new mathematical transform inspired by the physics of photonic time stretch. We showed via analytical derivations and numerical simulations that the so called Phase Stretch Transform equalizes the input brightness resulting in a high dynamic range in feature detection and acts as a hyper-dimensional feature set classifier. Furthermore, our results show a method for the computation of mathematical derivatives via group delay dispersion operations

ACKNOWLEDGMENT

H. Asghari was with the Department of Electrical and Computer Engineering, University of California Los Angeles, Los Angeles, CA, USA.

REFERENCES

[1] B. S. Manjunath, C. Shekhar, and R. Chellappa, "A new approach to image feature detection with applications," *Pattern Recognit.*, vol. 29, no. 4, pp. 627–640, Apr. 1996.
[2] B. Zitová and J. Flusser, "Image registration methods: A survey," *Image Vis. Comput.*, vol. 21, pp. 977–1000, Oct. 2003.
[3] Y. LeCun, Y. Bengio, and G. Hinton, "Deep learning," *Nature*, vol. 521, no. 7553, pp. 436–444, May. 2015.
[4] G. Medioni and R. Nevatia, "Matching images using linear features," *IEEE Trans. Pattern Anal. Mach. Intell.*, vol. PAMI-6, no. 6, pp. 675–685, Nov. 1984.
[5] H. Stokman and T. Gevers, "Selection and fusion of color models for image feature detection," *IEEE Trans. Pattern Anal. Mach. Intell.*, vol. 29, no. 3, pp. 371–381, Mar. 2007.
[6] J. van de Weijer, T. Gevers, and A. D. Bagdanov, "Boosting color saliency in image feature detection," *IEEE Trans. Pattern Anal. Mach. Intell.*, vol. 28, no. 1, pp. 150–156, Jan. 2006.
[7] T. Lindeberg, "Feature detection with automatic scale selection," *Int. J. Comput. Vis.*, vol. 30, no. 2, pp. 79–116, 1998.
[8] M. Pavlić, H. Belzner, G. Rigoll, and S. Ilić, "Image based fog detection in vehicles," in *Proc. 4th Intell. Veh. Symp.*, Jun. 2012, pp. 1132–1137.

[9] S. Sivaraman and M. M. Trivedi, "Looking at vehicles on the road: A survey of vision-based vehicle detection, tracking, and behavior analysis," *IEEE Trans. Intell. Transp. Syst.*, vol. 14, no. 4, pp. 1773–1795, Dec. 2013.
[10] M. H. Asghari and B. Jalali, "Physics-inspired image edge detection," in *Proc. IEEE Global Conf. Signal Inf. Process.*, Dec. 2014, pp. 293–296.
[11] M. H. Asghari and B. Jalali, "Edge detection in digital images using dispersive phase stretch transform," *J. Biomed. Imag.*, vol. 2015, Jan. 2015, Art. no. 6.
[12] A. S. Bhushan, F. Coppinger, and B. Jalali, "Time-stretched analogue-to-digital conversion," *Electron. Lett.*, vol. 34, no. 11, pp. 1081–1082, May. 1998.
[13] Y. Han and B. Jalali, "Photonic time-stretched analog-to-digital converter: Fundamental concepts and practical considerations," *J. Lightw. Technol.*, vol. 21, no. 12, p. 3085, Dec. 2003.
[14] W. Ng, T. Rockwood, and A. Reamon, "Demonstration of channel-stitched photonic time-stretch analog-to-digital converter with ENOB 8 for a 10 GHz signal bandwidth," in *Proc. GOMACTech*, 2014, p. 26.2.
[15] A. Mahjoubfar, C. L. Chen, and B. Jalali, "Design of warped stretch transform," in *Artificial Intelligence in Label-Free Microscopy*. Berlin, Germany: Springer, 2017, pp. 101–119.
[16] A. Mahjoubfar, D. V. Churkin, S. Barland, N. Broderick, S. K. Turitsyn, and B. Jalali, "Time stretch and its applications," *Nature Photon.*, vol. 11, no. 6, pp. 341–351, 2017.
[17] D. R. Solli, C. Ropers, P. Koonath, and B. Jalali, "Optical rogue waves," *Nature*, vol. 450, no. 7172, pp. 1054–1057, Dec. 2007.
[18] C. Szwaj *et al.*, "Unveiling the complex shapes of relativistic electrons bunches, using photonic time-stretch electro-optic sampling," in *Proc. IEEE Photon. Soc. Summer Topical Meeting Ser.*, Jul. 2016, pp. 136–137.
[19] C. L. Chen *et al.*, "Deep learning in label-free cell classification," *Sci. Rep.*, vol. 6, Mar. 2016, Art. no. 21471.
[20] A. Mahjoubfar, C. L. Chen, and B. Jalali, *Artificial Intelligence in Label-Free Microscopy: Biological Cell Classification by Time Stretch*. Berlin, Germany: Springer, 2017.
[21] C. L. Chen, A. Mahjoubfar, and B. Jalali, "Optical data compression in time stretch imaging," *PLoS ONE*, vol. 10, no. 4, p. e0125106, 2015.
[22] B. Jalali, M. Suthar, M. Asghari, and A. Mahjoubfar, "Optics-inspired Computing," in *Proc. 5th Int. Conf. Photon., Opt. Laser Technol.*, vol. 1. 2017, pp. 340–345, doi: 10.5220/0006271703400345.
[23] B. Jalali and A. Mahjoubfar, "Tailoring wideband signals with a photonic hardware accelerator," *Proc. IEEE.*, vol. 103, no. 7, pp. 1071–1086, Jul. 2015.
[24] M. Suthar, A. Mahjoubfar, K. Seals, E. W. Lee, and B. Jalali, "Diagnostic tool for pneumothorax," in *Proc. Photon. Soc. Summer Topical Meeting Ser.*, Jul. 2016, pp. 218–219.
[25] C. V. Ilioudis, C. Clemente, M. H. Asghari, B. Jalali, and J. J. Soraghan, "Edge detection in SAR images using phase stretch transform," in *Proc. 2nd IET Int. Conf. Intell. Signal Process.*, Dec. 2015, pp. 1–5.
[26] T. Ilovitsh, B. Jalali, M. H. Asghari, and Z. Zalevsky, "Phase stretch transform for super-resolution localization microscopy," *Biomed. Opt. Exp.*, vol. 7, no. 10, pp. 4198–4209, Oct. 2016.
[27] *Jalali Lab UCLA/Image-Feature-Detection-Using-Phase-Stretch-Transform*. [Online]. Available: https://github.com/JalaliLabUCLA/Image-feature-detection-using-Phase-Stretch-Transform/
[28] Z. Hameed and C. Wang, "Edge detection using histogram equalization and multi-filtering process," in *Proc. IEEE Int. Symp. Circuits Syst.*, May 2011, pp. 1077–1080.

MADHURI SUTHAR (S'16) received the B.Tech. degree in electronics and communication engineering from the Indian Institute of Technology-Indian School of Mines Dhanbad (IIT-ISM Dhanbad), India, in 2014, the M.S. degree with thesis in electrical engineering from the University of California at Los Angeles (UCLA), USA, in 2016. She is currently pursuing the Ph.D. degree in electrical engineering at UCLA, under the supervision of Prof. B. Jalali. As an undergraduate researcher she has worked at Indian Institute of Technology (IIT)-Bombay (India), The University of British Columbia, Vancouver, Canada, and IBM, Bangalore, India. Her research interests include image and signal processing, machine learning, optics and photonics. Prof. Suthar is currently a Co-Organizer of Optical Data Science: Trends Shaping the Future of Photonics Conference in SPIE Photonics West/OPTO 2018. Since 2016, she has been holding the position of treasurer for OSA-SPIE student chapter at UCLA. She has received the Student of the Year Award for securing highest GPA in the institute among all branches at IIT-ISM Dhanbad. She was the Gold Medalist for securing rank one in her institute during undergraduate studies.

HOSSEIN ASGHARI is with the Electrical Engineering and Computer Science Department, Loyola Marymount University, as an Assistant Professor. His scientific contributions have resulted in three international patents, one U.S. patent, ten provisional patents, 14 invited seminars, one book, and 71 publications in high-impact international journals and conferences including 11 invited and post-deadline papers. He is a member of the Optical Society of America (OSA). His scientific works have been high-lighted multiple times in well-recognized international magazines. Prof. Asghari has received numerous prizes, honors and recognitions from USA, Canada, and international agencies. This includes the UCLA Chancellor's Award for Post-Doctoral Research in 2014, honored annually to six post-doctoral researchers among 1,167 post-doctoral positions in all of the departments. He was a recipient of the NSERC and FQRNT Post-Doctoral Fellowships in 2011 from the Government of Canada and Quebec Government, respectively. His contribution on Anamorphic data compression received the Best Paper Award in the IEEE International Symposium on Image Processing (ISSPT 2013). He is the Chair of Los Angeles Chapter of IEEE Photonics Society. He is also a Co-Organizer of the Conference on Real-time Measurements, Rogue Events, and Emerging Applications, in SPIE Photonics West/OPTO 2016. He was a Co-Organizer and the Co-Chair of the symposium on Information processing for Big Data, the IEEE Global Conference on Signal and Information Processing (IEEE GlobalSIP 2014). He was also a Co-Organizer and the Co-Chair of the annual Danish-Californian photonic workshop in connection with Optical Fiber Communication Conference (OFC 2015) supported by the Danish Innovation Center, Denmark. He has served as the General Co-Chair of sub-conferences in SPIE 2014 and PIERS 2014 conferences. He was a Reviewer of OSA Student Chapter Excellence Awards in 2012. Prof. Asghari is a reviewer of top scientific journals, including the *Nature Photonics, Optics Letters*, the *Optics Express*, and the IEEE JOURNAL OF LIGHTWAVE. He holds an FQRNT Doctoral Fellowship from the Quebec Government, Canada.

BAHRAM JALALI (F'12) is the Northrop-Grumman Chair in optoelectronics and a Professor of electrical engineering with the University of California at Los Angeles (UCLA) with joint appointments in Biomedical Engineering and in the UCLA David Geffen School of Medicine. He is an Inventor of the photonic time stretch and other high speed imaging and sensing methodologies that have been commercialized. Prof. Jalali was a recipient of the R. W. Wood Prize from the Optical Society of America for the invention and demonstration of the first Silicon Laser, and the Aron Kressel Award of the IEEE Photonics Society, the IET Achievement Medal, and the Distinguished Engineering Achievement Award from the Engineers Council. He is a fellow of the Optical Society of America, the American Physical Society, and SPIE.